Redox Biology 59 (2023) 102557

Contents lists available at ScienceDirect

Redox Biology

journal homepage: www.elsevier.com/locate/redox

Myeloperoxidase-derived hypochlorous acid targets human airway epithelial plasmalogens liberating protein modifying electrophilic 2-chlorofatty aldehydes

Shubha Shakya [a,b], Kelly D. Pyles [a,b], Carolyn J. Albert [a,b], Rakesh P. Patel [c,d], Kyle S. McCommis [a,b], David A. Ford [a,b,*]

[a] Edward A. Doisy Department of Biochemistry and Molecular Biology, Saint Louis University School of Medicine, St. Louis, MO, 63104, USA
[b] Center for Cardiovascular Research, Saint Louis University School of Medicine, St. Louis, MO, 63104, USA
[c] Department of Pathology, University of Alabama at Birmingham, Birmingham, AL, 35294, USA
[d] Center for Free Radical Biology, University of Alabama at Birmingham, Birmingham, AL, 35294, USA

ARTICLE INFO

Keywords:
Chlorinated lipids
Protein modification
Proteomics
Myeloperoxidase

ABSTRACT

Neutrophil and airway epithelial cell interactions are critical in the inflammatory response to viral infections including respiratory syncytial virus, Sendai virus, and SARS-CoV-2. Airway epithelial cell dysfunction during viral infections is likely mediated by the interaction of virus and recruited neutrophils at the airway epithelial barrier. Neutrophils are key early responders to viral infection. Neutrophil myeloperoxidase catalyzes the conversion of hydrogen peroxide to hypochlorous acid (HOCl). Previous studies have shown HOCl targets host neutrophil and endothelial cell plasmalogen lipids, resulting in the production of the chlorinated lipid, 2-chlorofatty aldehyde (2-ClFALD). We have previously shown that the oxidation product of 2-ClFALD, 2-chlorofatty acid (2-ClFA) is present in bronchoalveolar lavage fluid of Sendai virus-infected mice, which likely results from the attack of the epithelial plasmalogen by neutrophil-derived HOCl. Herein, we demonstrate small airway epithelial cells contain plasmalogens enriched with oleic acid at the *sn-2* position unlike endothelial cells which contain arachidonic acid enrichment at the *sn*-2 position of plasmalogen. We also show neutrophil-derived HOCl targets epithelial cell plasmalogens to produce 2-ClFALD. Further, proteomics and over-representation analysis using the ω-alkyne analog of the 2-ClFALD molecular species, 2-chlorohexadecanal (2-ClHDyA) showed cell adhesion molecule binding and cell-cell junction enriched categories similar to that observed previously in endothelial cells. However, in contrast to endothelial cells, proteins in distinct metabolic pathways were enriched with 2-ClFALD modification, particularly pyruvate metabolism was enriched in epithelial cells and mitochondrial pyruvate respiration was reduced. Collectively, these studies demonstrate, for the first time, a novel plasmalogen molecular species distribution in airway epithelial cells that are targeted by myeloperoxidase-derived hypochlorous acid resulting in electrophilic 2-ClFALD, which potentially modifies epithelial physiology by modifying proteins.

1. Introduction

Neutrophils are the first responders of infection [1–3]. Neutrophils combat viral infections by phagocytosis, degranulation, respiratory burst and release of neutrophil extracellular traps [4]. Despite its role in removing viral particles, the presence of neutrophils in different viral infections such as respiratory syncytial virus [5,6], SARS-CoV-2 virus [7] and Sendai virus [8] has shown to be deleterious to epithelial cells. Understanding the interaction of neutrophils and epithelial cells is vital for better therapeutic approaches to limit lung injury. Neutrophil myeloperoxidase converts hydrogen peroxide to hypochlorous acid (HOCl). HOCl is a potent two-electron oxidant that reacts with viral as well as host DNA, proteins, and lipids [9–13]. HOCl targets the plasmalogen phospholipid vinyl ether bond liberating the vinyl ether masked aldehyde as 2-chlorofatty aldehyde (2-ClFALD) [14]. We have previously shown that neutrophil-derived HOCl targets endothelial plasmalogens leading to 2-ClFALD production [14]. Subsequently, we have

* Corresponding author. Edward A. Doisy Department of Biochemistry and Molecular Biology, Saint Louis University School of Medicine, 1100 Grand Blvd., DRC 325, St. Louis, MO, 63104, USA.
E-mail address: david.ford@health.slu.edu (D.A. Ford).

https://doi.org/10.1016/j.redox.2022.102557
Received 15 November 2022; Accepted 25 November 2022
Available online 7 December 2022

Abbreviations

HOCl	hypochlorous acid
2-ClFALD	2-chlorofatty aldehyde
2-ClHDA	2-chlorohexadecanal
2-ClHDyA	2-chlorohexadec-y-nal
2-ClFA	2-chlorofatty acid
HLMVEC	human lung microvascular endothelial cell
HSAEC	human small airway epithelial cell
ESI MS/MS	electrospray ionization tandem mass spectrometry
HDyA	hexadec-y-nal
GC/MS	gas chromatography mass spectrometry
LPE	lysophosphatidylethanolamine;
MPO	myeloperoxidase
PC	choline glycerophospholipid
PE	ethanolamine glycerophospholipid
PMA	phorbol 12-myristate 13-acetate
WebGestalt	Web-based gene set analysis toolkit
Panther	Protein analysis through evolutionary relations
BP	biological process
MF	molecular function
CC	cellular component
KEGG	Kyoto Encyclopedia of Genes and Genomes

demonstrated 2-ClFALD modifies a number of endothelial cell proteins in human lung microvascular endothelial cells (HLMVEC) [15]. Although the 2-ClFALD oxidation product, 2-chlorofatty acid (2-ClFA), is found in bronchoalveolar lavage fluid (BALF) fluid [16], it is not clear whether the plasmalogen source is from lung endothelium or epithelium.

In addition to the targeting of plasmalogens by HOCl, the antioxidant properties of plasmalogens may have far ranging roles in the lung since this organ is directly exposed to many environmental exposures including pathogens and chemical agents [17–19]. Plasmalogens are present in lung surfactant, epithelial cells, and endothelial cells [17,20–22], where they act as the first line of defense against oxidants [17,18]. Plasmalogens are glycerophospholipids with an acid labile vinyl ether bond that is targeted by oxidants [23,24]. Typically, plasmalogens contain an acyl group at the *sn-2* group enriched in arachidonic acid (AA) and docosahexaenoic acid, C22:6 ω−3 (DHA). Plasmalogens serve as a storage depot for AA [25]. AA is the substrate for a number of lipid mediators that play an important role in inflammation and immune response [26]. In general, plasmalogens contain either a choline or ethanolamine polar head group at the *sn*-3 position of the glycerol backbone. The ethanolamine plasmalogens, plasmenylethanolamines, are found in many organs and cell types [27]. In the present study, we have characterized the plasmalogen content in human small airway epithelial cells (HSAEC) and demonstrated that they are targeted by neutrophil derived HOCl. Furthermore, using click chemistry analogs of 2-chlorofatty aldehyde we show that the proteome modified by 2-ClFALD in HSAEC are distinct compared to those modified in HLMVEC. Finally, we show that 2-ClFALD targets proteins that regulate pyruvate metabolism resulting in decreased mitochondrial pyruvate respiration.

2. Materials and Methods

2.1. Materials

Cell culture supplies were purchased from Sigma-Aldrich (St. Louis, MO, USA). Click chemistry reagents were purchased from Click Chemistry Tools, (Scottsdale, AZ, USA). All other chemicals were purchased from Sigma-Aldrich (St. Louis, MO, USA) or Thermo Fisher Scientific (Waltham, MA, USA). The 2-ClFALD molecular species, 2-chlorohexadecanal (2-ClHDA) ω-alkyne analog (2-ClHDyA) was synthesized as previously described [15,28–30].

2.2. Cell culture

Human small airway epithelial cell (HSAEC) (Lonza, CC-2547, Basel, Switzerland) were grown in SAGM™ BulletKit™ (Lonza, cat. CC-3118, Basel, Switzerland) in 5% CO_2/95% air at 37 °C. Human lung microvascular endothelial cells (HLMVEC) (PromoCell cat. C12281, Heidelberg, Germany) were grown in EGM-2MV (Lonza, cat. CC-3202, Basel, Switzerland) in 5% CO_2/95% air at 37 °C. Under these growth conditions the media pyruvate and glucose concentrations are 0.6 mM and 6 mM, respectively, for HSAEC; and 1.2 and 5.5 mM, respectively, for HLMVEC.

2.3. Lipid analysis

HSAEC and HLMVEC were grown to confluency in six-well plates. Lipids were extracted using Bligh and Dyer extraction in the presence of lipid class internal standards containing phosphatidylethanolamine (PE) (14:0–14:0, xx:y-xx:y indicate the number of carbons (x) and number of double bonds (y) in the *sn*-1 and *sn*-2 aliphatic groups, respectively), and phosphatidylcholine (PC) (20:0–20:0). Lipidomics were performed on Q Exactive mass Spectrometer (Thermo Fisher Scientific, Waltham, MA, USA) or Triple quadrupole instrument Altis (Thermo Fisher Scientific, Waltham, MA, USA) equipped with Vanquish UHPLC system as described previously [31]. Briefly, lipids were separated on an Accucore C18 column 2.1 × 150 mm with mobile phase A comprised of 60% acetonitrile, 40% water, 10 mM ammonium formate and 0.1% formic acid and mobile phase B comprised of 90% isopropanol, 10% acetonitrile, 2 mM ammonium formate and 0.02% formic acid and analyzed using selected reaction monitoring as described previously [31]. Fatty acid molecular species were derivatized to their pentafluorobenzyl esters and subsequently were quantitated by GC-MS as previously described [32,33].

2.4. Neutrophil and epithelial cell transwell culture chamber studies

Neutrophils were isolated from whole blood of healthy human donors with approval by the Saint Louis University Institutional Review Board. Briefly, whole blood was centrifuged over a density gradient. After centrifugation, the polymorphonuclear cell band was isolated and washed with Hanks's balanced salt solution (HBSS). The red blood cells were lysed and neutrophils were washed twice with HBSS before preparing relevant neutrophil concentrations in HBSS. HSAEC were grown to confluency in six well culture plates. Cells were washed in warm phosphate-buffered saline immediately prior to experiments. Transwell chambers containing a polyethylene terephthalate membrane pore size 0.4 μm were inserted into the wells in the presence and absence of PMA stimulated neutrophils (1×10^7) above HSAEC (about 2×10^5 cells). After a 30 min incubation, transwell chambers were removed. Lipids were extracted in presence of 2-Cl-*[d_4]*-HDA from HSAEC for 2-ClFALD measurements by GC-MS following derivatization of the lipid extracts to prepare the PFB oxime of 2-ClHDA as previously described [34,35]. A separate analysis was performed with lipids extracted in presence of PE (14:0/14:0) and LPE (14:0) using Bligh Dyer method [36]. HSAEC lipids were subsequently analyzed using the lipidomics platform described above.

2.5. Click reactions of 2-ClHDyA-modified proteins with biotin-azide

Proteins targeted by 2-ClHDyA in HSAEC cells were pulled down and identified as previously described [15]. Briefly, HSAEC were grown to confluency in T75 flasks with SABM media (Lonza, CC-3119, Basel, Switzerland) and SAGM™ SingleQuots™ supplements (Lonza, CC-4123, Basel, Switzerland). The cells were then washed and treated with 10 μM HDyA or 10 μM 2-ClHDyA or vehicle (DMSO only) in 11 mL SABM for 1 h at 37 °C. After 1 h, cells were washed, and lysed with 750 μL RIPA with 1X cOmplete mini EDTA-free protease inhibitor cocktail and 400 μM PMSF. Protein lysates were precleared for natural biotinylated proteins using high-capacity streptavidin-agarose beads. 500 μg protein was used for click chemistry. Proteins were diluted to 750 μL PBS. Subsequently, 100 μM of azide-biotin was added, followed by 90 μL of water, 40 μL of 150 μM THPTA, and 60 μL of a 1:5 ratio mixture of 150 mM THPTA: 30 mM Cu(II)SO_4 and 50 μL of 400 mM sodium ascorbate were added. Samples were subsequently rocked for 30 min at room temperature. Excess click reagents were removed by using 10 mL Zeba 7 K MW cutoff desalting columns (Thermo Fisher Scientific, cat. 89893, Waltham, MA, USA) equilibrated in DPBS, as per the manufacturer's instructions. NP-40 (final concentration of 1%), SDS (final concentration 0.1%), PMSF (final concentration 400 μM) and cOmplete mini protease inhibitor cocktail (final concentration (1X)) was added to the eluent to prevent protein degradation. A total of ~175 μg of cleaned biotin-azide clicked proteins were incubated with 30 μL of high-capacity streptavidin-agarose beads overnight at 4 °C with rotation. The beads were washed sequentially with 0.15% NP-40 (four times on ice), 6 M urea in 50 mM Tris pH 8.0 (4 times, 15 min, with rotation at 4 °C), 2 mM $CaCl_2$ in 50 mM Tris pH 8.0 (4 times, 15 min on ice). Washed streptavidin beads were then subjected to either SDS-PAGE or proteomics analysis.

2.6. LC-MS/MS analysis of captured proteins

Biotin-azide clicked proteins bound to streptavidin-agarose beads were subjected to on-bead trypsin digestion, peptide clean-up and proteomic analysis by LC-MS/MS as previously described [15]. Briefly, proteins (230 μL) were reduced with 2.3 μL of 500 mM freshly made DTT at 56 °C for 30 min, followed by alkylation with 4.6 μL of 1 M iodoacetamide (IAA) for 30 min in the dark. Excess IAA was quenched with an additional DTT for 5 min at room temperature. Reduced and alkylated biotin-tagged proteins were digested with 500 ng of trypsin (Promega, cat. V5111, Madison, WI, USA) for 20 h at 37 °C by shaking at 1400 rpm. The tryptic peptides were purified and concentrated with C18 columns (Thermo Fisher Scientific, cat. 89870, Waltham, MA, USA), according to the manufacturer's protocol. The eluted peptides were dried and subsequently resuspended in 40 μL water/acetonitrile/formic acid (98/2/0.1). Samples were analyzed on a Thermo Q Exactive orbitrap MS/MS equipped with a nanospray emitter (Thermo Fisher Scientific, Waltham, MA, USA). Nanospray parameters in positive ion mode were as follows: spray voltage, 2.0 kV; capillary temperature, 320 °C; S-lens RF level, 55. Liquid chromatography was performed on a Dionex™ UltiMate™ 3000 RSLC (Thermo Fisher Scientific, Waltham, MA, USA). Mobile phase A consisted of 0.1% formic acid in water and mobile phase B consisted of 80% acetonitrile in water with 0.1% formic acid. Samples were loaded onto the loading column in 2% acetonitrile in water with 0.1% formic acid present. The peptides were separated by reversed-phase chromatography on a C18 nano column (Acclaim PepMap C18 HPLC column 15 cm × 75 μm, 2 μm particles, 100 Å pore size, Thermo Fisher Scientific, Waltham, MA, USA) at a flow rate of 300 nL/min. The column temperature was maintained at 35 °C. The peptide samples were injected onto the column at 99% A, which was held for 3 min, followed by a linear gradient from 1% to 65% B over 90 min. Subsequently, hydrophobic peptides were step eluted over 1 min with 90% B, which was held for 4 min. Columns were subsequently re-equilibrated with 99% A for 22 min. The top 10 peptides were selected in a data-dependent mode for MS/MS fragmentation by collision-induced dissociation. The automatic gain control (AGC) target was set to 3×10^6 with resolution 70,000 and maximum injection time 100 ms. For MS2 analysis, the AGC target mode was set to 5×10^4 with a maximum injection time of 100 ms and a resolution of 17,500. The isolation window was set to 1.8 *m/z*. Collision energy of −28 eV was used to fragment ions. Analysis was performed with a dynamic exclusion of 40.0 s and charge exclusion of unassigned, 1, 6–8, and >8.

2.7. Proteomic analysis of peptides of captured proteins

The identification of the peptides and proteins was performed on Proteome Discoverer 2.4.1.15 with processing and consensus workflows as described previously [15]. Briefly, MS/MS spectra were analyzed using Sequest HT and MSPepSearch, both integrated into Proteome Discoverer 2.4.1.15 (Thermo Fisher Scientific, Waltham, MA, USA). The Swiss-Prot (version: 2017-10-25, accessed 04-20-2021, St. Louis, MO, USA) database for *Homo sapiens* was used to search the data in Sequest HT. The NIST Human Orbitrap spectral library (NIST_Human_Orbitrap_HCD_20160923, version 1.0, accessed 09-07-2018, St. Louis, MO, USA) and ProteomeTools_HCD30_PD (version 1.0, accessed 10-16-2018, St. Louis, MO, USA) were used to search data with MSPepsearch. The results were subjected to statistical analysis using the percolator node where the false discovery rate (FDR) was calculated using a decoy database search, and only high confidence peptide identifications with FDR <0.01 were included. Identifications were accepted only for proteins with greater than one peptide identification and five PSMs. Further, accepted proteins that were present in nine of twelve replicates were used for gene ontology analysis.

2.8. Gene ontology analysis

Gene ontology analysis was performed using Web-based gene set analysis toolkit WebGestalt 2019 as previously described [15]. Briefly, we entered the UniProt accession ID of protein targets into the WebGestalt 2019, accessed several times during 04–2021 to 05–2022) [37–41]. We chose over-representation analysis as the enrichment method for gene ontology (Molecular Function (MF), Biological Process (BP), and Cellular Component (CC)) and Kyoto Encyclopedia of Genes and Genomes (KEGG) pathway. *Homo sapiens* was selected as the organism. The reference list was analyzed against the genome protein coding reference set. The parameters for the enrichment analysis for 2-ClHDyA-specific hits included the minimum number of IDs in the category [5], the maximum number of IDs in the category (2000), the Bonferroni correction method and FDR ($p < 0.05$). Additionally, protein analysis through evolutionary relations (Panther) was used to identify the protein classes [42,43]. No FDR was used for Panther analysis.

2.9. SDS-PAGE and western blotting

SDS-PAGE as well as Streptavidin probed Western blot were performed as previously described [15].

2.10. Mitochondrial respiration

Mitochondrial oxygen consumption rate (OCR) was assessed with a Seahorse XFe96 analyzer (Agilent, Santa Clara, CA) using the Agilent mitochondrial stress test according to the manufacturer's procedures. Briefly, HSAEC cells were seeded at 1.0×10^4 cells per well in an XFe96 cell cartridge plate (Agilent, Santa Clara, CA) and incubated in normal media overnight. The next day, the cells were treated with DMSO (Vehicle), or 10 μM 2-ClHDyA in their normal media with no FBS for 1 h at 37 °C. The treatment was performed in n = 18. After vehicle or 2-ClHDyA treatment, media was switched to Seahorse DMEM supplemented with 10 mM Glucose and 1 mM pyruvate, and incubated in a non-CO_2 incubator at 37 °C for 1 h. Assay injections were performed at the following concentrations: oligomycin at 1 μM, 2-{2-[4-

(trifluoromethoxy)phenyl]hydrazinylidene}-propanedinitrile (FCCP) at 2 μM, and antimycin A/rotenone at 1 μM.

2.11. Statistics analysis

ANOVA with the Sidak multiple comparison test was used for comparison between two groups in Fig. 3. All data are presented as mean ± SEM unless otherwise noted. Data in Figs. 1, 2 and 7 were analyzed by *t*-test.

3. Results

3.1. Distribution of plasmalogen in HSAEC and HLMVEC

Initial studies compared the plasmalogen content of HSAEC to HLMVEC. Fig. 1A and B shows the total and molecular species plasmenylcholine content, respectively, of these two human primary lung cells. A striking difference is the content of oleic acid esterified to the *sn*-2 position of plasmenylcholine in HSAEC compared to HLMVEC as illustrated in Fig. 1C. For both HSAEC and HLMVEC there is approximately 3-fold more plasmenylethanolamine compared to plasmenylcholine (Figs. 2A and 1A). Similar to plasmenylcholine, HSAEC plasmenylethanolamine was enriched with oleic acid in the *sn*-2 position compared to HLMVEC plasmenylethanolamine, which was enriched with arachidonic acid at the *sn-2* position (Fig. 2B and C). HSAEC and HLMVEC growth media were examined for the content of oleic acid and arachidonic acid (Fig. 2D), which showed while there nearly equal amounts of these fatty acids in the HLMVEC media, HSAEC media contained ~2-fold more oleic acid compared to arachidonic acid.

3.2. Neutrophil-derived HOCl target HSAEC plasmalogens

Data shown in Fig. 3A indicate plasmenylethanolamine molecular species including the abundant species with oleic acid at the *sn-2* position are targeted by neutrophil-derived HOCl. These studies were performed with HSAEC plated below transwells containing human neutrophils under control or PMA-stimulated conditions. Similar to our past studies with endothelial cells, these data indicate HOCl produced in a transwell above cells can diffuse and attack HSAEC plasmalogens. Data in Fig. 3B show the lysophosphatidylethanolamine levels under these conditions. The lysophosphatidylethanolamine product of HOCl targeting plasmenylethanolamine molecular species containing *sn*-2 oleic acid is significantly increased by PMA stimulated neutrophils. Additionally, Fig. 3C shows both 2-chlorohexadecanal and 2-chlorooctadecanal accumulate in the HSAEC cells under conditions of PMA-activated neutrophils in the transwell compartment.

3.3. Protein targets of 2-ClHDyA in HSAEC

2-ClFALD-modified proteins were identified as described previously with HLMVEC [15]. HSAEC were treated with either 2-ClHDyA, HDyA, or vehicle (DMSO) for 1 h at 37 °C ($n = 3$). 2-ClHDyA is the click chemistry analog of 2-ClHDA, a 2-ClFALD molecular species. Unreacted 2-ClHDyA was removed from the media and modified HSAEC proteins were clicked with biotin-azide. Biotinylated proteins were pulled down using streptavidin agarose beads. Following streptavidin-agarose bead enrichment of modified proteins, eluted biotinylated proteins were separated and visualized in SDS-PAGE using silver stain (Fig. 4A). As well as with streptavidin-HRP binding (Fig. 4B). Tryptic peptides generated by on-bead digestion were analyzed by LC-MS/MS. The peptides and their corresponding proteins were identified with

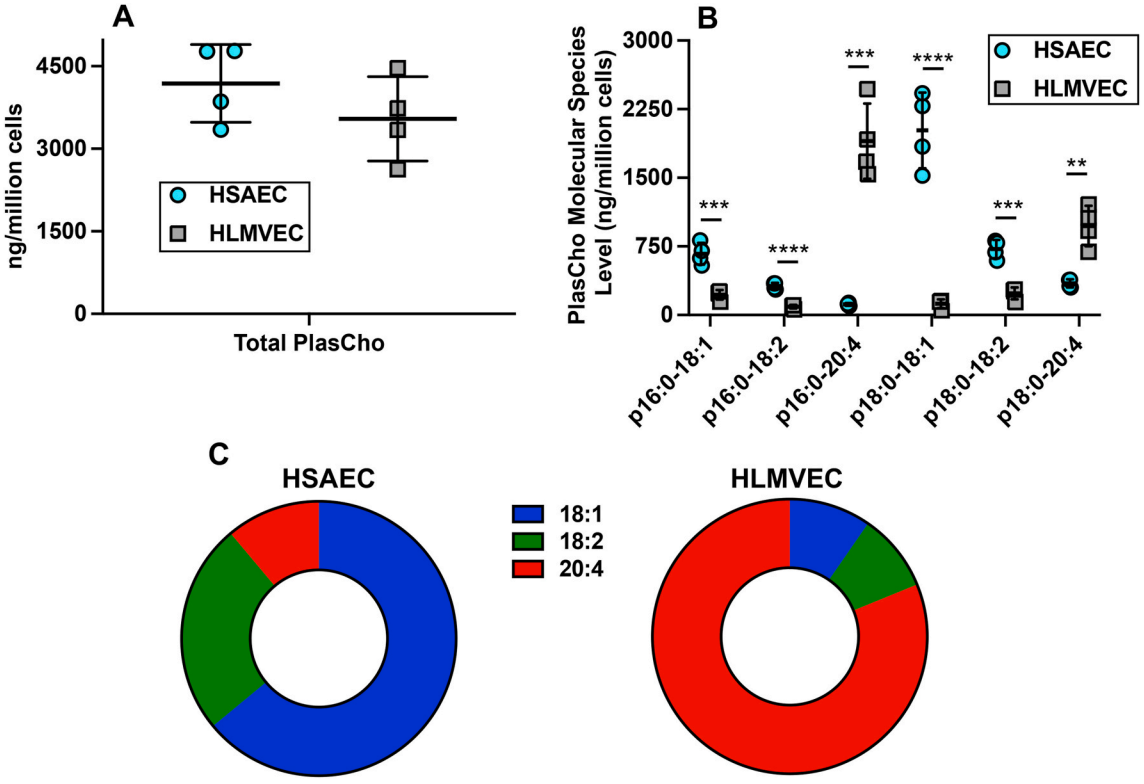

Fig. 1. Distribution of Plasmenylcholine Molecular Species in HSAEC and HLMVEC: Cells were grown to confluence on six well plates. Lipids were extracted and analyzed for plasmenylcholine (PlasCho) molecular species by PRM using QE MS/MS as described in "Materials and Methods". Total PlasCho (A) in HSAEC and HLMVEC was further analyzed for different molecular species (B). **, ***, and **** indicate $p < 0.01$, 0.001, and 0.0001, respectively. p designates plasmalogen molecular species. 18:1, 18:2, and 20:4 indicate oleic, linoleic, and arachidonic acid aliphatic groups in the *sn*-2 position, respectively, of HSAEC and HLMVEC PlasCho. Panel C shows the distribution of *sn*-2 aliphatic constituents in PlasCho of HSAEC and HLMVEC.

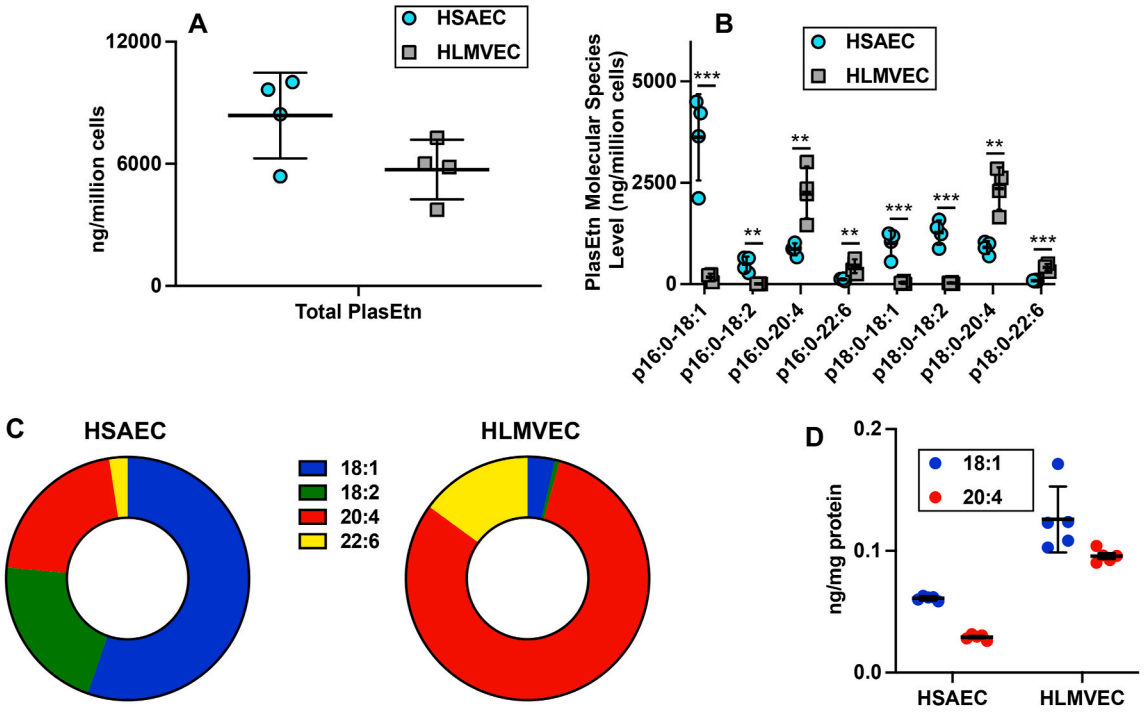

Fig. 2. Distribution of Plasmenylethanolamine Molecular Species in HSAEC and HLMVEC: Cells were grown to confluence on six-well plates. Lipids were extracted and analyzed for plasmenylethanolamine (PlasEtn) molecular species by PRM using QE MS/MS as described in "Materials and Methods". Total PlasEtn (A) in HSAEC and HLMVEC was further analyzed for different molecular species (B). ** and *** indicate $p < 0.01$ and 0.001, respectively. p designates plasmalogen molecular species. 18:1, 18:2, 20:4, and 22:6 indicate oleic, linoleic, arachidonic, and docosahexaenoic acid aliphatic groups in the *sn*-2 position, respectively, of HSAEC and HLMVEC PlasEtn. Panel C shows the distribution of *sn*-2 aliphatic constituents in PlasEtn of HSAEC and HLMVEC. Panel D: Oleic acid and arachidonic acid content in HSAEC and HLMVEC media.

Proteome Discoverer 2.4.1.15, using the Sequest HT and MSPepSearch databases. Only matches that met the defined criteria, as described in the "Materials and Methods", were accepted. A total of 728 proteins were modified by 2-ClHDyA (Fig. 4C). Among these 728 proteins, 349 proteins were specifically modified by 2-ClHDyA (i.e., they were not modified by HDyA). And the remaining 379 proteins were modified by both 2-ClHDyA and HDyA. These two groups of proteins were separately entered into the Panther database to determine their distribution in protein classes (Fig. 5A, **6A**). The most targeted protein classes modified by 2-ClHDyA alone as well as 2-ClHDyA and HDyA were the metabolite interconversion enzyme class and protein modifying enzyme class. WebGestalt was used to perform over-representation analysis (ORA). Fig. 5B–D and **6B, D, E** show the enriched categories (FDR <0.05) associated with biological processes, cellular components, and molecular functions, respectively. Additionally, Figs. 5E and 6C show enriched KEGG pathways. A complete list of the HSAEC proteins modified by 2-ClHDyA alone (Table S1) and both 2-ClHDyA and HDyA (Table S2) and 2-ClHDyA and/or HDyA (Table S3) are in the supplementary tables. Although a number of proteins are identified to be modified by HDyA, non-chlorinated analog, with respect to the intensity of biotinylation in 2-ClHDyA elute sample in Western blot (Fig. 4B), it should be noted that the proteins identified in the HDyA sample are probably modified in multiple amino acids by 2-ClHDyA leading to the increased intensity of the blot in Fig. 4B.

Since 2-ClHDA is produced by activated neutrophils during infection, it is interesting that the neutrophil-mediated immunity, granulocyte activation, ficolin-1-rich granule (granule specific to neutrophil) and bacterial invasion of epithelial cells are enriched in both gene ontology and KEGG pathways. A list of proteins in these categories are listed in supplementary tables (Table S4, **S5**, **S6**, and **S7**). Other major gene ontology and KEGG pathways that were enriched with proteins modified by 2-ClHDyA in HSAEC included the proteosome pathway, cell adhesion mediator activity pathway and cell adhesion binding molecule pathway (Table S8, **S9** and **S10**). One of the enriched KEGG pathways in HSAEC was pyruvate metabolism. Proteins belonging to pyruvate metabolism are listed in the supplementary table (Table S11). One of the proteins modified by 2-ClHDyA is pyruvate dehydrogenase E1 alpha 1, which is important for mitochondrial respiration.

3.4. 2-ClHDyA-mediated alteration in HSAEC mitochondrial respiration

Since the pyruvate metabolism KEGG pathway was modified by 2-ClHDyA in HSAEC cells, we investigated the effects of this lipid on mitochondrial respiration. Oxygen consumption rates of HSAECs provided with glucose and pyruvate and subjected to mitochondrial inhibitor protocols are shown in Fig. 7A. Basal respiration (Fig. 7B) was similar in 2-ClHDyA- and DMSO-treated cells. However, 2-ClHDyA-treated cells displayed a significantly lower response to ATP synthase inhibitor, oligomycin, indicating less respiration being coupled to ATP production (Fig. 7A, **C**). Proton leak calculated by the difference between non-mitochondrial respiration and ATP-linked respiration as well as maximum respiration capacity were not altered by 2-ClHDyA treatment (Fig. 7A, **D, 7E**). Fig. 7F shows extracellular acidification rate (ECAR) data from these studies, which suggest differences, albeit not significant, in basal ECAR under these condition, with differences reduced during the mitochondrial stress tests with oligomycin, FCCP and rotenone. Alterations in ATP-linked respiration are suggested by our findings that 2-ClHDyA modifies proteins related to pyruvate metabolism (Table S11).

4. Discussion

Neutrophil-epithelial cell interactions have been shown to be important in different viral conditions such as respiratory syncytial virus [5,6], SARS-CoV-2 [7] and Sendai virus [8]. Sendai virus has been shown to cause neutrophilic bronchiolitis [8] and leads to increases in

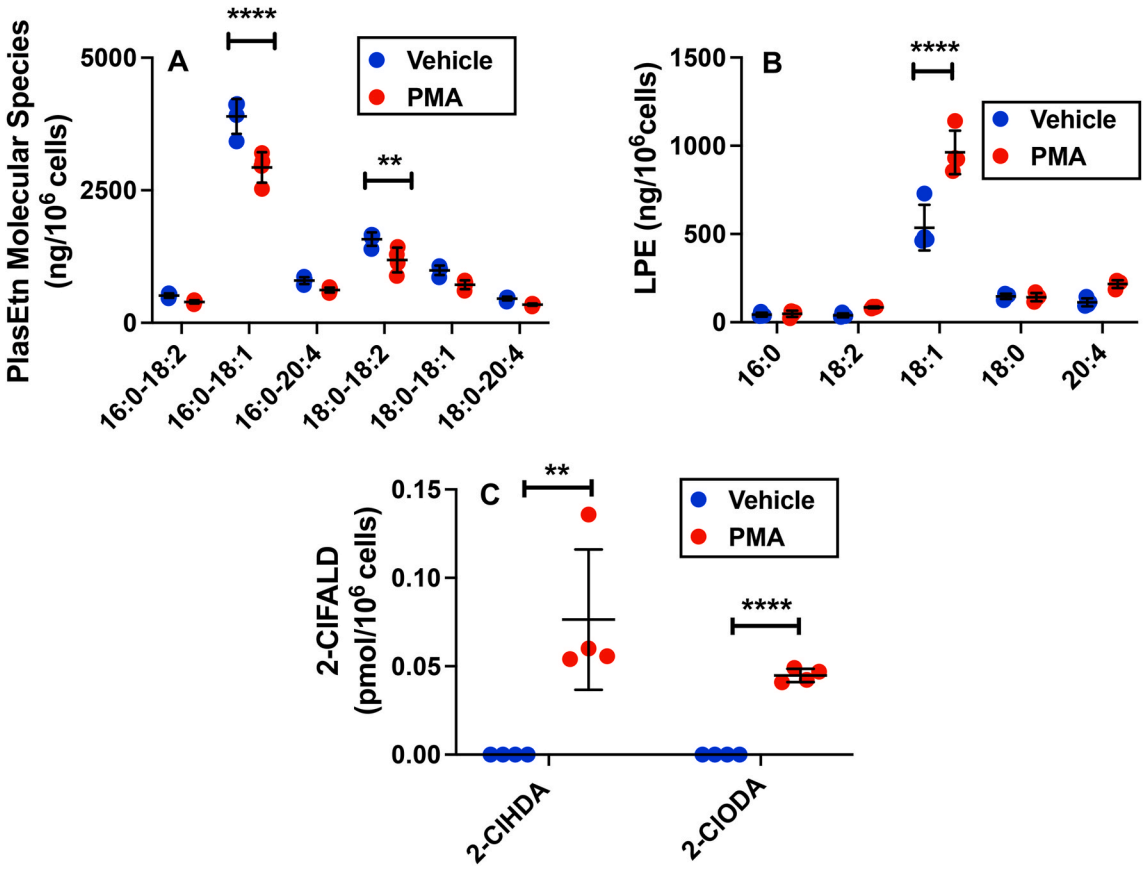

Fig. 3. Neutrophil-derived HOCl target HSAEC plasmalogen and produce 2-ClFALD. Confluent HSAEC were grown on six-well plates with transwell inserts in presence and absence of PMA activated neutrophils for 30 min at 37 °C. After incubation, transwell inserts were removed. Lipids associated with HSAEC were extracted and analyzed for PlasEtn molecular species (A), lysophosphatidylethanolamine (LPE) molecular species (B) and 2-ClFALD molecular species (C) as described in "Materials and Methods". All data are presented in mean ± SD. ****p<0.0001, **p<0.01.

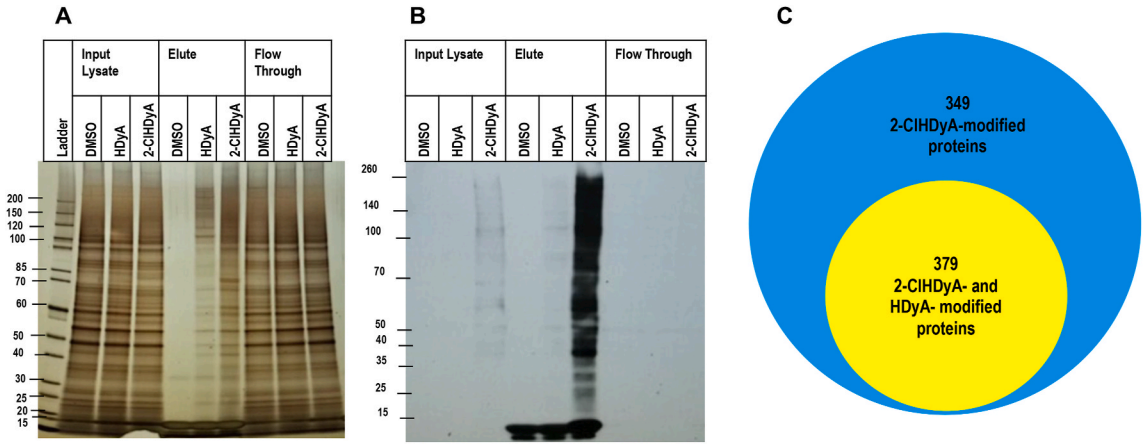

Fig. 4. 2-ClHDyA modified HSAEC proteins. Protein pull down samples from indicated conditions were subjected to SDS-PAGE and silver staining (A) and Western blotting (B) probed with streptavidin HRP as described in "Materials and Methods". Protein loads showing total proteins from lysates from each indicated condition (DMSO vehicle, HDyA (non-chlorinated aldehyde control) and 2-ClHDyA) input onto beads, elute from beads, and supernatant (Flow Through); (C) Venn diagram of the number of 2-ClHDyA- and HDyA-modified proteins in HSAEC cells.

2-chlorofatty acid levels in plasma and BALF of infected mice [16]. The presence of 2-ClFA in BALF suggests interaction of neutrophil derived HOCl and epithelial cells. Previously we have shown that neutrophil-derived reactive chlorinating species target endothelial plasmalogens to produce 2-ClFALD, which can covalently modify endothelial cell proteins [14,15] Herein, we show the primary human small airway epithelial cells, HSAEC, have a unique distribution of plasmalogens molecular species that are enriched with oleic acid at the *sn*-2 position, compared to the enrichment of arachidonic acid in HLMVEC. The difference in plasmalogens containing oleic acid and arachidonic acid may in part reflect a 2-fold increase in oleic acid in the HSAEC growth media compared to that in the HLMVEC growth media. We also demonstrated HSAEC plasmalogens are targeted by myeloperoxidase-derived HOCl to produce 2-ClFALD. These data

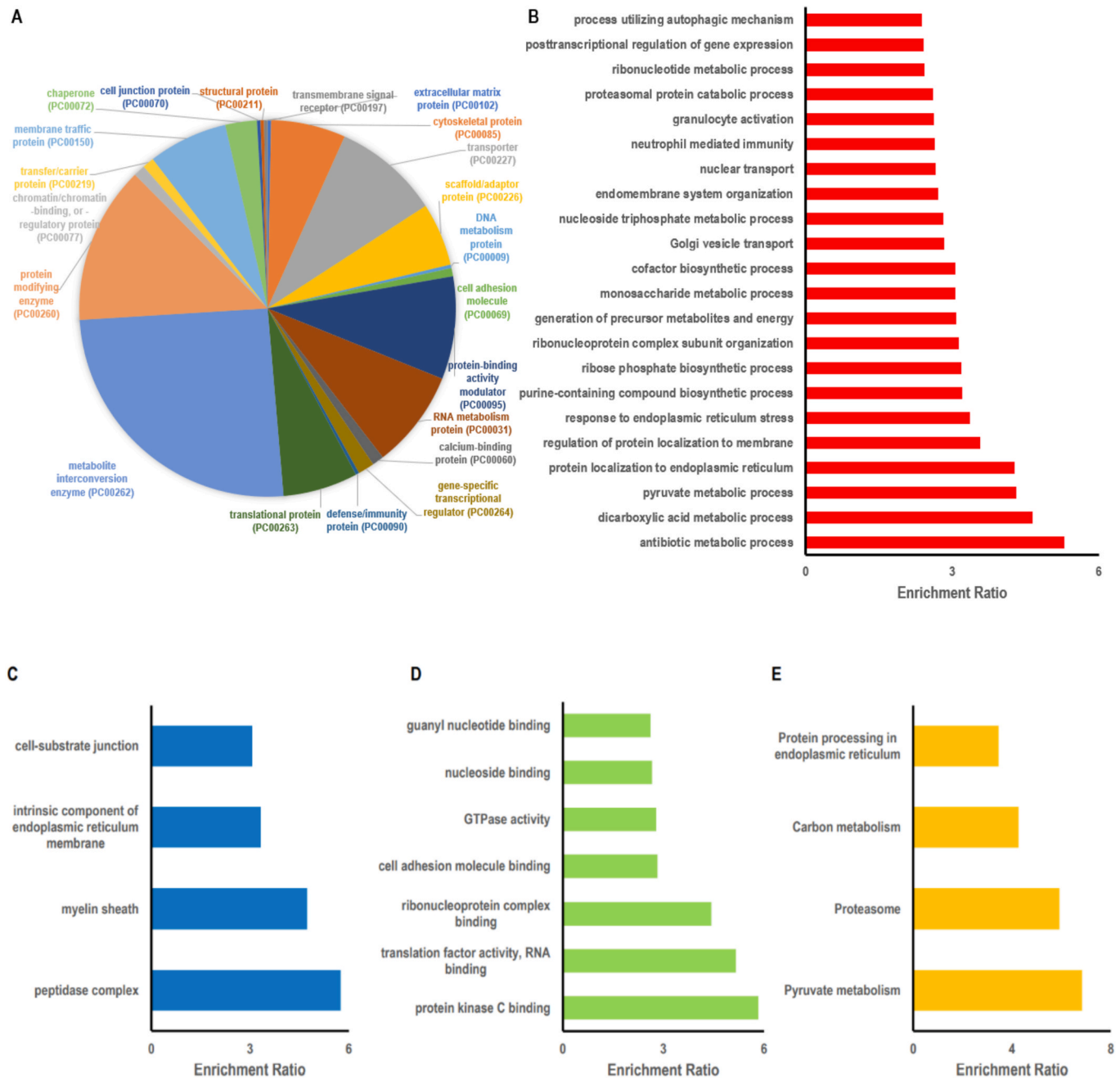

Fig. 5. Bioinformatic characterization of HSAEC proteins modified by 2-ClHDyA: (A) Distribution of 2-ClHDyA-modified proteins by protein class analyzed using Panther; (B–E) Over-representation analysis using the Web-based Gene Set Analysis Toolkit (WebGestalt). Enriched categories in Gene Ontology (GO) Biological function (B); Cellular component (C); Molecular function (D); and KEGG Pathway using Bonferroni $p < 0.05$ for computing FDR ($p < 0.05$) (E).

support the likelihood that 2-ClFA found in BALF of Sendai virus-infected mice [16] is derived from epithelial 2-ClFALD conversion to 2-ClFA [15,16,44].

Plasmalogens are important glycerophospholipids that are present in different mammalian tissue including lungs [21,45–48]. Plasmalogens contain a vinyl ether bond at *sn-1* position and are enriched in polyunsaturated fatty acids, specifically DHA, or AA at *sn-2* position [26,49–51]. AA and DHA are substrates for synthesis of different lipid mediators including prostaglandins, thromboxanes, leukotrienes and resolvins [26]. In our studies, we found HSAEC plasmalogens are enriched with oleic acid. We speculate that the enrichment of oleic acid in airway epithelium may reflect the primary role of this lipid as a component of secreted surfactant [22], while endothelial plasmalogens may have a greater role in the production of bioactive oxylipid production.

We have previously shown 2-ClFALD reacts with glutathione [52] and proteins [15,28,53]. Furthermore, we applied click chemistry followed by streptavidin agarose bead pull-down to identify the protein targets of 2-ClFALD. Seven hundred and twenty-eight proteins were shown to be modified by 2-ClHDyA including those modified by HDyA in HSAEC. A total of 6841 proteins have been reported to be identified in human bronchial epithelial cell [54]. Thus, about 11% of HSAEC proteins are modified by 2-ClHDyA. It is possible that additional proteins could be modified by 2-ClFALD formed endogenously. These proteins may not be detected by the addition of hydrophobic exogenous 2-ClHDyA, which may have limited accessibility to redox sensitive cysteines. In comparison only 6% of EA.hy926 cells were found to be modified by 2-ClHDyA [15]. Among 728 proteins, 379 proteins were

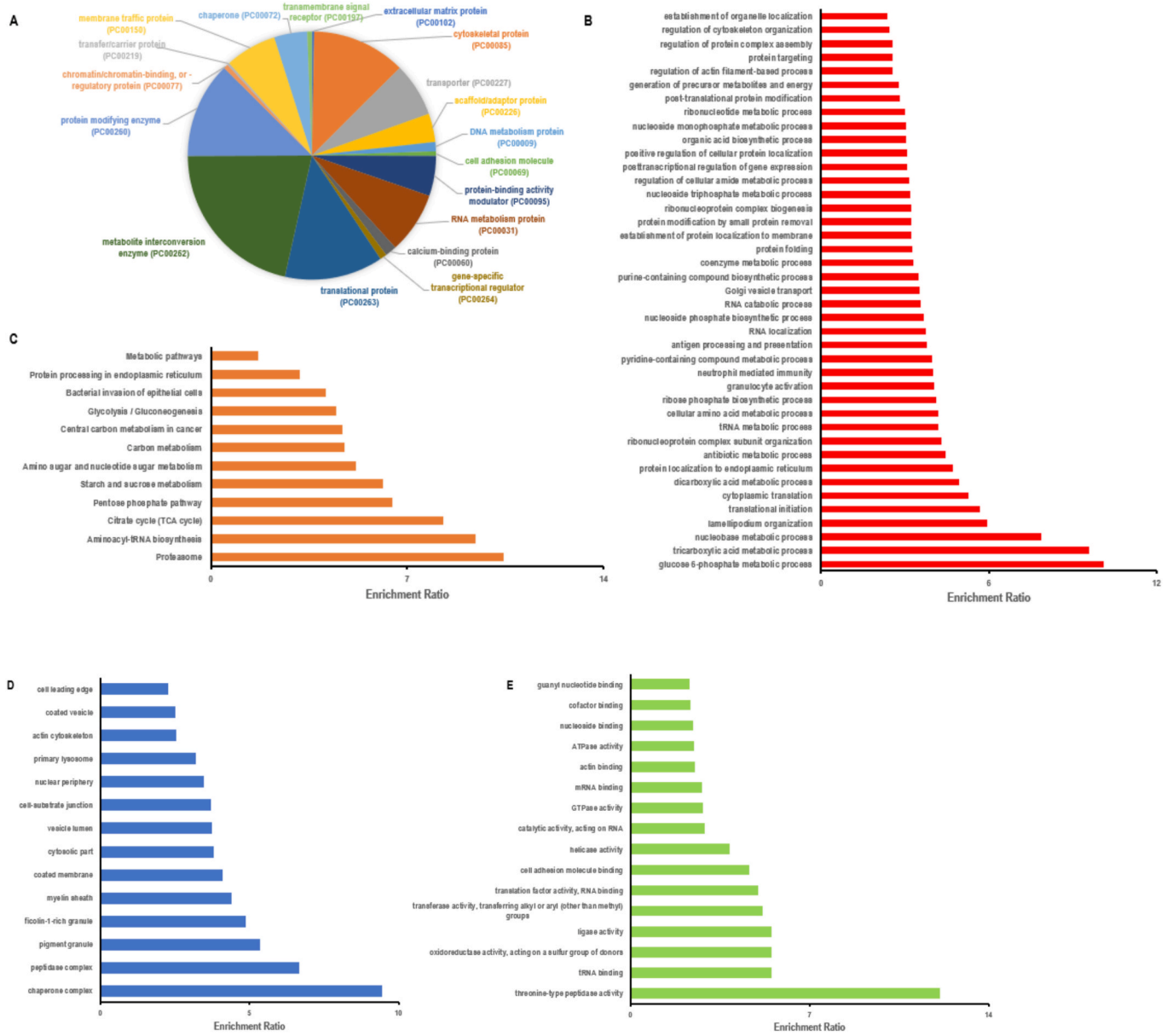

Fig. 6. Bioinformatic characterization of HSAEC proteins modified by 2-ClHDyA and HDyA: (A) Distribution of 2-ClHDyA-modified proteins by protein class analyzed using Panther; (B–E) Over-representation analysis using the Web-based Gene Set Analysis Toolkit (WebGestalt). Enriched categories in Gene Ontology (GO) Biological function (B); Cellular component (D); Molecular function (E); and KEGG Pathway using Bonferroni $p < 0.05$ for computing FDR ($p < 0.05$) (C).

also modified by HDyA suggesting nonspecific binding by these lipids. Similar to endothelial cells, metabolite interconversion enzyme and protein modifying enzyme groups were most abundantly represented in the HSAEC proteins modified by 2-ClHDyA (Fig. 5A, **6A**).

Previous studies have demonstrated that 2-ClFALD causes endothelial barrier dysfunction [29,55]. 2-ClFALD has also been shown to cause blood-brain barrier dysfunction [53,56,57]. Endothelial cells and epithelial cells share similar junctional proteins with tight junction and adherens junction being the two major groups [58]. Recently, we found that GO biological processes cell junction organization, molecular function cell adhesion molecule binding, and KEGG pathway adherens junction were significantly enriched among the proteins modified by 2-ClHDyA in HLMVEC. As expected, there is strong overlap between proteins modified by 2-ClHDyA in HSAEC and HLMVEC. These include molecular function cell adhesion molecule binding and cell adhesion mediator binding are also significantly enriched among the proteins modified by 2-ClHDyA in HSAEC (Figs. 5 and 6). Similar to the endothelial cells, KEGG pathway proteosome is also significantly enriched among the proteins targeted by 2-ClHDyA in HSAEC which might be involved in β-catenin-dependent adherens junction leakiness [59]. Additionally, different catenins (α-catenin, p120-catenin, γ-catenin, and β-catenin) which play an important role in barrier function, were targeted by 2-ClFALD similar to endothelial cell, suggesting 2-ClHDyA might mediate epithelial barrier dysfunction via protein modification. One difference between proteins modified in HSAEC and HLMVEC related to barrier function are the desmosome proteins, which are modified in HSAEC, but not HLMVEC. This difference between the cells is due to the absence of desmosomes in endothelial cell [60]. Although there is major overlap of proteins modified in both HSAEC and HLMVEC that are related to barrier function it is possible that proteins modified in the desmosome could lead to specific mechanisms 2-ClHDyA alters airway epithelial barrier function.

A number of metabolism pathways were significantly enriched in HSAEC which were not significantly enriched in endothelial cells [15].

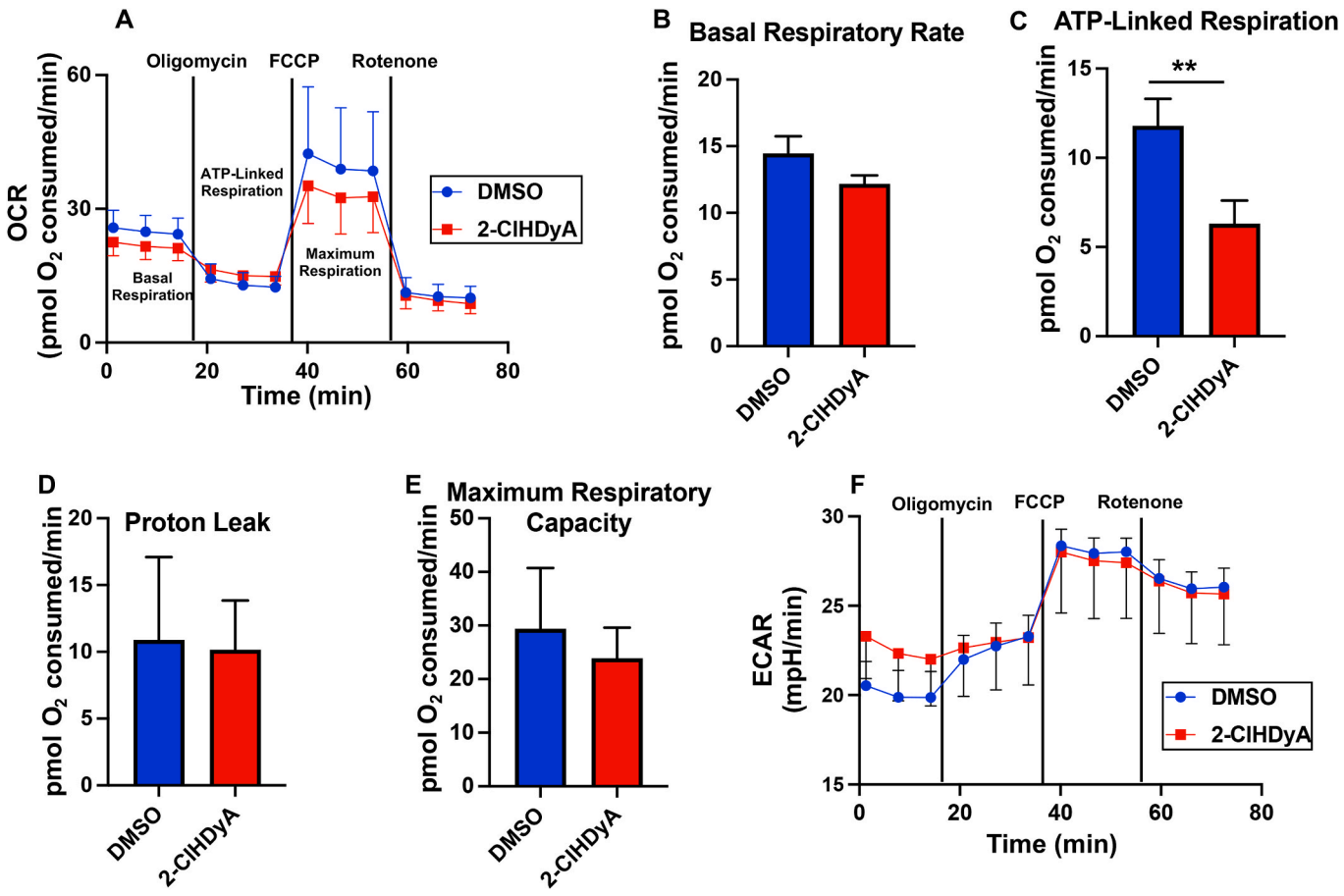

Fig. 7. The effect of 2-ClHDyA on mitochondrial respiration: HSAEC were treated with DMSO or 2-ClHDyA as described in "Materials and Methods". (A) Diagram showing the oxygen consumption rate (OCR) throughout the series of mitochondrial inhibitor injections. (B) Basal HSAEC respiration on glucose and pyruvate 1 h after removal of 2-ClHDyA or DMSO. (C–E) Measurement of respiration rates after various inhibitors of the electron transport chain. (F) Diagram showing the extracellular acidification rate (ECAR) throughout the series of mitochondrial inhibitor injections. All data are presented as mean ± SEM for n = 3 independent experiments. Data were analyzed by unpaired *t*-test compared to the DMSO treatment. $^{**}p < 0.01$.

In particular, the pyruvate metabolism pathway was enriched. A recent proteomics study on epithelial and endothelial cells showed a preferential enrichment of proteins in the GO biological process groups including lipid biosynthetic process, fatty acid metabolic process and oxidation-reduction [22]. The greater proportion of metabolic processing pathways in epithelial cells provides some rationale to the enrichment of metabolic processing pathway enzymes that are covalently modified by 2-ClHDyA. Further 2-ClHDyA decreased mitochondrial respiration and specifically the efficiency of coupling oxygen consumption with ATP generation. Interestingly, 2-ClHDyA-treated cells also failed to increase glycolysis rates (ECAR) after being treated with the ATP synthase inhibitor oligomycin. While lactate dehydrogenase were not specifically modified by 2-ClHDyA, monocarboxylate transporters and several ATP synthase subunits were modified (Tables S1 and S2), which may be responsible for this result. This uncoupling may lead to compromised cellular function especially during stress. This possibility, together with the mechanisms underlying inhibited mitochondrial respirations in HSAEC treated with 2-ClHDyA requires further study.

5. Conclusion

Altogether, we demonstrate epithelial cells contain a unique composition of plasmalogen that is different from endothelial cells. Neutrophil-derived reactive oxygen species target epithelial cell plasmalogen to produce 2-ClFALD, which modifies epithelial proteins and can alter mitochondrial respiration. In comparison to our previous studies showing human lung microvascular endothelial cell protein modification by 2-ClFALD, more proteins are modified by 2-ClFALD in human small airway epithelial cells including an abundance of proteins related to metabolic processing. Proteomics data suggest many pathways are potentially altered due to the 2-ClFALD covalent modification of key pathway proteins, as identified in our studies employing the click chemistry analog of 2-ClFALD, 2-ClHDyA. This data rich study indicates there are many pathways that need to be examined to improve our understanding of mechanisms altered by 2-ClFALD production. We initiated interrogation of these pathways in this study by demonstrating pyruvate mitochondrial ATP production is decreased by 2-ClHDyA treatment. Altogether this study provides insights into novel interactions of neutrophils and epithelial cells through HOCl targeting plasmalogens and 2-ClFALD production leading to protein modification impacting many cellular and metabolic processes.

Funding

This study was supported (in part) by research funding from the National Institutes of Health R01 GM-115553, R21 ES-031562, R01 ES-034383 and S10OD025246 to DAF. The content is solely the responsibility of the authors and does not necessarily represent the official views of the National Institutes of Health.

Appendix A. Supplementary data

Supplementary data to this article can be found online at https://doi.

org/10.1016/j.redox.2022.102557.

References

[1] T. Németh, M. Sperandio, A. Mócsai, Neutrophils as emerging therapeutic targets, Nat. Rev. Drug Discov. 19 (2020) 253–275.
[2] Bart W. Bardoel, Elaine F. Kenny, G. Sollberger, A. Zychlinsky, The balancing act of neutrophils, Cell Host Microbe 15 (2014) 526–536.
[3] C. Rosales, Neutrophil: a cell with many roles in inflammation or several cell types? Front. Physiol. 9 (2018).
[4] Y. Ma, Y. Zhang, L. Zhu, Role of neutrophils in acute viral infection, Immun. Inflamm. Dis. 9 (2021) 1186–1196.
[5] Y. Deng, J.A. Herbert, E. Robinson, L. Ren, R.L. Smyth, C.M. Smith, Neutrophil-airway epithelial interactions result in increased epithelial damage and viral clearance during respiratory syncytial virus infection, J. Virol. 94 (2020), e02161-02119.
[6] Y. Deng, J.A. Herbert, C.M. Smith, R.L. Smyth, An in vitro transepithelial migration assay to evaluate the role of neutrophils in Respiratory Syncytial Virus (RSV) induced epithelial damage, Sci. Rep. 8 (2018) 6777.
[7] B.A. Calvert, E.J. Quiroz, Z. Lorenzana, N. Doan, S. Kim, C.N. Senger, W. D. Wallace, M.P. Salomon, J.E. Henley, A.L. Ryan, Neutrophil-epithelial interactions augment infectivity and pro-inflammatory responses to SARS-CoV-2 infection, bioRxiv (2021), 455472, 2021.2008.2009.
[8] L.P. Shornick, A.G. Wells, Y. Zhang, A.C. Patel, G. Huang, K. Takami, M. Sosa, N. A. Shukla, E. Agapov, M.J. Holtzman, Airway epithelial versus immune cell Stat1 function for innate defense against respiratory viral infection, J. Immunol. 180 (2008) 3319–3328.
[9] J.P. Eiserich, C.E. Cross, A.D. Jones, B. Halliwell, A. van der Vliet, Formation of nitrating and chlorinating species by reaction of nitrite with hypochlorous acid. A novel mechanism for nitric oxide-mediated protein modification, J. Biol. Chem. 271 (1996) 19199–19208.
[10] F.A. Villamena, Chemistry of Reactive Species, 2013.
[11] C.L. Hawkins, M.J. Davies, Hypochlorite-induced damage to DNA, RNA, and polynucleotides: formation of chloramines and nitrogen-centered radicals, Chem. Res. Toxicol. 15 (2002) 83–92.
[12] T.D. Oury, L. Tatro, A.J. Ghio, C.A. Piantadosi, Nitration of tyrosine by hydrogen peroxide and nitrite, Free Radic. Res. 23 (1995) 537–547.
[13] C.C. Winterbourn, J.J.M. van den Berg, E. Roitman, F.A. Kuypers, Chlorohydrin formation from unsaturated fatty acids reacted with hypochlorous acid, Arch. Biochem. Biophys. 296 (1992) 547–555.
[14] A.K. Thukkani, F.F. Hsu, J.R. Crowley, R.B. Wysolmerski, C.J. Albert, D.A. Ford, Reactive chlorinating species produced during neutrophil activation target tissue plasmalogens: production of the chemoattractant, 2-chlorohexadecanal, J. Biol. Chem. 277 (2002) 3842–3849.
[15] S. Shakya, R.A. Herr, H.L. Carlson, R.A. Zoeller, C.J. Albert, D.A. Ford, Endothelial Cell Protein Targeting by Myeloperoxidase-Derived 2-chlorofatty Aldehyde. Antioxidants (Basel), vol. 11, 2022.
[16] D.S. Anbukumar, L.P. Shornick, C.J. Albert, M.M. Steward, R.A. Zoeller, W. L. Neumann, D.A. Ford, Chlorinated lipid species in activated human neutrophils: lipid metabolites of 2-chlorohexadecanal, J. Lipid Res. 51 (2010) 1085–1092.
[17] R. Zhuo, P. Rong, J. Wang, R. Parvin, Y. Deng, The potential role of bioactive plasmalogens in lung surfactant, Front. Cell Dev. Biol. 9 (2021), 618102.
[18] K.M. Wynalda, R.C. Murphy, Low-concentration ozone reacts with plasmalogen glycerophosphoethanolamine lipids in lung surfactant, Chem. Res. Toxicol. 23 (2010) 108–117.
[19] D.A. Ford, J. Honavar, C.J. Albert, M.A. Duerr, J.Y. Oh, S. Doran, S. Matalon, R. P. Patel, Formation of chlorinated lipids post-chlorine gas exposure, J. Lipid Res. 57 (2016) 1529–1540.
[20] K.A. Berry, B. Li, S.D. Reynolds, R.M. Barkley, M.A. Gijón, J.A. Hankin, P. M. Henson, R.C. Murphy, MALDI imaging MS of phospholipids in the mouse lung, J. Lipid Res. 52 (2011) 1551–1560.
[21] E.J. Murphy, L. Joseph, R. Stephens, L.A. Horrocks, Phospholipid composition of cultured human endothelial cells, Lipids 27 (1992) 150–153.
[22] J.E. Kyle, G. Clair, G. Bandyopadhyay, R.S. Misra, E.M. Zink, K.J. Bloodsworth, A. K. Shukla, Y. Du, J. Lillis, J.R. Myers, J. Ashton, T. Bushnell, M. Cochran, G. Deutsch, E.S. Baker, J.P. Carson, T.J. Mariani, Y. Xu, J.A. Whitsett, G. Pryhuber, C. Ansong, Cell type-resolved human lung lipidome reveals cellular cooperation in lung function, Sci. Rep. 8 (2018), 13455.
[23] P.J. Sindelar, Z. Guan, G. Dallner, L. Ernster, The protective role of plasmalogens in iron-induced lipid peroxidation, Free Radic. Biol. Med. 26 (1999) 318–324.
[24] R.A. Zoeller, A.C. Lake, N. Nagan, D.P. Gaposchkin, M.A. Legner, W. Lieberthal, Plasmalogens as endogenous antioxidants: somatic cell mutants reveal the importance of the vinyl ether, Biochem. J. 338 (1999) 769–776.
[25] D.A. Ford, R.W. Gross, Plasmenylethanolamine is the major storage depot for arachidonic acid in rabbit vascular smooth muscle and is rapidly hydrolyzed after angiotensin II stimulation, Proc. Natl. Acad. Sci. U. S. A. 86 (1989) 3479–3483.
[26] N.E. Braverman, A.B. Moser, Functions of plasmalogen lipids in health and disease, Biochim. Biophys. Acta (BBA) - Mol. Basis Dis. 1822 (2012) 1442–1452.
[27] Y. Otoki, S. Kato, F. Kimura, K. Furukawa, S. Yamashita, H. Arai, T. Miyazawa, K. Nakagawa, Accurate quantitation of choline and ethanolamine plasmalogen molecular species in human plasma by liquid chromatography–tandem mass spectrometry, J. Pharmaceut. Biomed. Anal. 134 (2017) 77–85.
[28] M.A. Duerr, E.N.D. Palladino, C.L. Hartman, J.A. Lambert, J.D. Franke, C.J. Albert, S. Matalon, R.P. Patel, A. Slungaard, D.A. Ford, Bromofatty aldehyde derived from bromine exposure and myeloperoxidase and eosinophil peroxidase modify GSH and protein, J. Lipid Res. 59 (2018) 696–705.
[29] J. McHowat, S. Shakya, D.A. Ford, 2-Chlorofatty aldehyde elicits endothelial cell activation, Front. Physiol. 11 (2020).
[30] C.L. Hartman, M.A. Duerr, C.J. Albert, W.L. Neumann, J. McHowat, D.A. Ford, 2-Chlorofatty acids induce Weibel-Palade body mobilization, J. Lipid Res. 59 (2018) 113–122.
[31] K. Amunugama, M.J. Jellinek, M.P. Kilroy, C.J. Albert, V. Rasi, D.F. Hoft, M.G. S. Shashaty, N.J. Meyer, D.A. Ford, Identification of novel neutrophil very long chain plasmalogen molecular species and their myeloperoxidase mediated oxidation products in human sepsis, Redox Biol. 48 (2021), 102208.
[32] O. Quehenberger, A. Armando, D. Dumlao, D.L. Stephens, E.A. Dennis, Lipidomics analysis of essential fatty acids in macrophages, Prostaglandins Leukot. Essent. Fatty Acids 79 (2008) 123–129.
[33] T.Q. de Aguiar Vallim, E. Lee, D.J. Merriott, C.N. Goulbourne, J. Cheng, A. Cheng, A. Gonen, R.M. Allen, E.N.D. Palladino, D.A. Ford, T. Wang, A. Baldan, E.J. Tarling, ABCG1 regulates pulmonary surfactant metabolism in mice and men, J. Lipid Res. 58 (2017) 941–954.
[34] W.Y. Wang, C.J. Albert, D.A. Ford, Approaches for the analysis of chlorinated lipids, Anal. Biochem. 443 (2013) 148–152.
[35] B.K. Wacker, C.J. Albert, B.A. Ford, D.A. Ford, Strategies for the analysis of chlorinated lipids in biological systems, Free Radic. Biol. Med. 59 (2013) 92–99.
[36] E.G. Bligh, W.J. Dyer, A rapid method of total lipid extraction and purification, Can. J. Biochem. Physiol. 37 (1959) 911–917.
[37] B. Zhang, S. Kirov, J. Snoddy, WebGestalt: an integrated system for exploring gene sets in various biological contexts, Nucleic Acids Res. 33 (2005) W741–W748.
[38] J. Wang, D. Duncan, Z. Shi, B. Zhang, WEB-Based GEne SeT AnaLysis toolkit (WebGestalt): update 2013, Nucleic Acids Res. 41 (2013) W77–W83.
[39] S. Kirov, R. Ji, J. Wang, B. Zhang, Functional annotation of differentially regulated gene set using WebGestalt: a gene set predictive of response to ipilimumab in tumor biopsies, Methods Mol. Biol. 1101 (2014) 31–42.
[40] J. Wang, S. Vasaikar, Z. Shi, M. Greer, B. Zhang, WebGestalt 2017: a more comprehensive, powerful, flexible and interactive gene set enrichment analysis toolkit, Nucleic Acids Res. 45 (2017) W130–W137.
[41] Y. Liao, J. Wang, E.J. Jaehnig, Z. Shi, B. Zhang, WebGestalt 2019: gene set analysis toolkit with revamped UIs and APIs, Nucleic Acids Res. 47 (2019) W199–W205.
[42] H. Mi, A. Muruganujan, X. Huang, D. Ebert, C. Mills, X. Guo, P.D. Thomas, Protocol Update for large-scale genome and gene function analysis with the PANTHER classification system (v.14.0), Nat. Protoc. 14 (2019) 703–721.
[43] P.D. Thomas, M.J. Campbell, A. Kejariwal, H. Mi, B. Karlak, R. Daverman, K. Diemer, A. Muruganujan, A. Narechania, PANTHER: a library of protein families and subfamilies indexed by function, Genome Res. 13 (2003) 2129–2141.
[44] K.R. Wildsmith, C.J. Albert, D.S. Anbukumar, D.A. Ford, Metabolism of myeloperoxidase-derived 2-chlorohexadecanal, J. Biol. Chem. 281 (2006) 16849–16860.
[45] R.W. Gross, High plasmalogen and arachidonic acid content of canine myocardial sarcolemma: a fast atom bombardment mass spectroscopic and gas chromatography-mass spectroscopic characterization, Biochemistry 23 (1984) 158–165.
[46] R.W. Gross, Identification of plasmalogen as the major phospholipid constituent of cardiac sarcoplasmic reticulum, Biochemistry 24 (1985) 1662–1668.
[47] J.E. Vance, Lipoproteins secreted by cultured rat hepatocytes contain the antioxidant 1-alk-1-enyl-2-acylglycerophosphoethanolamine, Biochim. Biophys. Acta Lipids Lipid. Metabol. 1045 (1990) 128–134.
[48] E.J. Murphy, M.B. Schapiro, S.I. Rapoport, H.U. Shetty, Phospholipid composition and levels are altered in Down syndrome brain, Brain Res. 867 (2000) 9–18.
[49] D.A. Ford, R.W. Gross, Plasmenylethanolamine is the major storage depot for arachidonic acid in rabbit vascular smooth muscle and is rapidly hydrolyzed after angiotensin II stimulation, Proc. Natl. Acad. Sci. U.S.A. 86 (1989) 3479–3483.
[50] X. Han, R.W. Gross, Electrospray ionization mass spectroscopic analysis of human erythrocyte plasma membrane phospholipids, Proc. Natl. Acad. Sci. U.S.A. 91 (1994) 10635–10639.
[51] X. Han, R.A. Gubitosi-Klug, B.J. Collins, R.W. Gross, Alterations in individual molecular species of human platelet phospholipids during thrombin stimulation: electrospray ionization mass spectrometry-facilitated identification of the boundary conditions for the magnitude and selectivity of thrombin-induced platelet phospholipid hydrolysis, Biochemistry 35 (1996) 5822–5832.
[52] M.A. Duerr, R. Aurora, D.A. Ford, Identification of glutathione adducts of alpha-chlorofatty aldehydes produced in activated neutrophils, J. Lipid Res. 56 (2015) 1014–1024.
[53] C. Nusshold, A. Ullen, N. Kogelnik, E. Bernhart, H. Reicher, I. Plastira, T. Glasnov, K. Zangger, G. Rechberger, M. Kollroser, G. Fauler, H. Wolinski, B.B. Weksler, I. A. Romero, S.D. Kohlwein, P.O. Couraud, E. Malle, W. Sattler, Assessment of electrophile damage in a human brain endothelial cell line utilizing a clickable alkyne analog of 2-chlorohexadecanal, Free Radic. Biol. Med. 90 (2016) 59–74.
[54] H.-X. Wang, X.-H. Qin, J. Shen, Q.-H. Liu, Y.-B. Shi, L. Xue, Proteomic analysis reveals that placenta-specific protein 9 inhibits proliferation and stimulates motility of human bronchial epithelial cells, Front. Oncol. 11 (2021).
[55] H. Yu, M. Wang, D. Wang, T.J. Kalogeris, J. McHowat, D.A. Ford, R.J. Korthuis, Chlorinated lipids elicit inflammatory responses in vitro and in vivo, Shock 51 (2019) 114–122.
[56] A. Ullen, E. Singewald, V. Konya, G. Fauler, H. Reicher, C. Nusshold, A. Hammer, D. Kratky, A. Heinemann, P. Holzer, E. Malle, W. Sattler, Myeloperoxidase-derived oxidants induce blood-brain barrier dysfunction in vitro and in vivo, PLoS One 8 (2013), e64034.

[57] A. Ullen, G. Fauler, E. Bernhart, C. Nusshold, H. Reicher, H.J. Leis, E. Malle, W. Sattler, Phloretin ameliorates 2-chlorohexadecanal-mediated brain microvascular endothelial cell dysfunction in vitro, Free Radic. Biol. Med. 53 (2012) 1770–1781.
[58] G. Bazzoni, E. Dejana, Endothelial cell-to-cell junctions: molecular organization and role in vascular homeostasis, Physiol. Rev. 84 (2004) 869–901.
[59] H. Aberle, A. Bauer, J. Stappert, A. Kispert, R. Kemler, β-catenin is a target for the ubiquitin-proteasome pathway, EMBO J. 16 (1997) 3797–3804.
[60] R. Werner, M.R. Gabor, Morphogenesis of Endothelium, CRC Press, Amsterdam, The Netherlands, 2000.